Applied Innovative Research
Vol. 1, June 2019, pp. 135-142

Study on stress-strain constitutive relationship of super-long-age plastic concrete under triaxial compression

Liangming Hu[a], Junfu Zhu[a*], Xin Jia[a], Changhui Zhang[b] & Danying Gao[a]
[a]College of Water Resources and Environment, Zhengzhou University, Zhengzhou-450001, China
[b]North China University of Water Resources and Electric Power, Zhengzhou-450045, China

Received 12 April 2019; accepted 19 June 2019

The triaxial stress-strain relationship of super long-aged (540d) plastic concrete mixed with clay and bentonite has been studied. According to the test, the stress-strain curves of plastic concrete under different confining pressures are obtained. It is found that the stress-strain curves under the lateral confining pressure are the same (0.4 MPa, 0.6 MPa), (0.4 MPa, 0.8 MPa), and the slope of the rising section is basically the same. Compared with the peak pressure ratio (0.2 MPa, 0.4 MPa), the lateral confining pressure is larger. In addition, the calculation formula of the peak secant elastic modulus and the triaxial compressive stress-strain relationship in accordance with the lateral pressure of plastic concrete have also been proposed. The fourth-order polynomial mathematical model. The establishment of the mathematical model provides a basis for the development of plastic concrete specifications and triaxial compression performance numerical analysis, and further promotes the engineering application of plastic concrete.

Keywords: Plastic concrete, Constitutive relation, Triaxial compression, Stress-strain relationship, Ultra-long age

1 Introduction

Plastic concrete is made by adding materials such as clay, bentonite, fly ash and other admixtures to concrete to enhance plasticity and reduce strength. Because of its good impermeability and deformation performance, in recent years, water conservancy and damming and engineering and high-rise building foundation anti-seepage projects have been widely used[1,2]. In engineering applications, plastic concrete is usually in a three-dimensional compression state, and the principal stress values in three directions are different ($\sigma_1 \neq \sigma_2 \neq \sigma_3$). Due to the complex nature of the plastic concrete constituent materials, it is more realistic and reasonable to directly determine the multiaxial mechanical properties of the plastic concrete by the test method[3]. Therefore, it is necessary to carry out a triaxial test that reflects the true mechanical properties of concrete.

There are many triaxial tests carried out for ordinary concrete both at home and abroad[4–6]. For plastic concrete, foreign expert Mahboubi *et al.*[7], conducted a triaxial compression test on plastic concrete. The study shows that the shear strength and cohesion of plastic concrete have a positive correlation with age, and the internal friction angle is opposite[7]. Nicholas *et al*., carried out an experimental study on the carbon fiber reinforced plastic concrete panels and established I-type fatigue model Hinchberger *et al*., carried out experimental research and theoretical analysis on the basic mechanical properties of plastic concrete, the causes of crack formation, the calculation of crack depth, and the prevention of crack propagation[9-13]. And the International Dam Conference suggested that the elastic modulus of the plastic concrete should be 1~ 5 times of the elastic modulus of the surrounding soil[14]. The domestic Tsinghua University scholar Deng Mingji combined with the Dongping Lake anti-seepage project to study the uniaxial compression mechanical properties of clay plastic concrete and bentonite plastic concrete[15]. Wang Xuanzi of Nanchang University studied the basic mechanical properties, working performance and durability of plastic concrete[16]. Domestic scholars Shi Yan and others studied the mechanical and triaxial stress-strain relationship of plastic concrete with low liquid limit clay, and found that the strength of plastic concrete decreases with the increase of clay content[17]. Shuaiqi *et al.,* studied The mechanical and impermeability properties of ash-plastic concrete in cement kiln[18]; Lulu *et al.,* studied the stress-strain characteristics of plastic concrete under cyclic loading and unloading[19].

*Corresponding author (E-mail: liangmingh@zzu.edu.cn)

In general, there are few true triaxial compression tests for plastic concrete. In this paper, the constitutive relationship of super-long-age plastic concrete mixed with clay and bentonite under triaxial compression is studied, and the triaxial compression constitutive relation is established. The fourth-order polynomial mathematical model has important theoretical significance and practical application value for the study of plastic concrete.

2 Experimental Procedure

2.1 Test raw materials

The experiment uses 42.5 # ordinary portland cement, calcium bentonite produced in Pingqiao Henan Xinyang, silty clay in the lake area of Longzi lake in Zhengdong new district, Zhengzhou city. The silty clay is retrieved and dried and ground to powder at a standard of 350 particle size. All the above indicators are in accordance with Ordinary Portland Cement[20] (GB175-2007) . The coarse aggregate used in the test is crushed stone with particle size of 5 ~ 20 mm. The fine aggregate is natural river sand, and the fineness modulus is 2.7. It belongs to medium sand and the grading curve is in the second zone. The aggregates meet the requirements of sand for construction[21] (GB/T14684－2011) and specifications for hydraulic concrete construction[22] (DL/T5144－2001) standards.

2.2 Design scheme of mix proportions of plastic concrete

In this experiment, clay and bentonite were used to replace part of the cement, and clay-bentonite-cement plastic concrete was made. The mass ratio method was used to design the mixture ratio. The sand ratio, water-to-binder ratio and unit water consumption were the three clear parameters in this test. The sand ratio is the ratio of the mass between sand and the total sand; the water-to-binder ratio is an indicator reflecting the ratio of the quality of water to cementitious materials (cement, bentonite and clay); the unit water consumption is the quality of the cement slurry and aggregate. After the trial distribution, the specific mix design was determined, as shown in Table 1.

2.3 Experimental method

According to the mixing ratio set in Table 1, 12 sets of 150 mm × 150 mm × 150 mm plastic concrete cube specimens were prepared, and the specimens were cured 540d under standard curing conditions after pouring.

This test uses a LY-C tensile true triaxial test for triaxial compression test. The test scheme is a triaxial compression test with a side pressure fixed. The triaxial compressive failure test is to apply a three-way pressure. The direction of σ_1 and σ_2 is increased to a predetermined confining pressure value, and the pressure is continuously applied to the concrete test in the direction of σ_3. Piece of damage, triaxial compressive strength is the peak of the stress-strain curve in the σ_3 direction. In this test, combined with engineering experience, three confining pressure conditions were established, namely σ_1=0.2MPa, σ_2=0.4MPa ; σ_1=0.4MPa, σ_2=0.6MPa ; σ_1=0.4MPa, σ_2=0.8MPa。 Let q = 1.0 MPa, simplified to (0.2q, 0.4q), (0.4q, 0.6q), (0.4q, 0.8q).

Table 1 — Mix proportions.

Number	Water binder ratio	Sand ratio	Water /kg	Cement content /kg	Clay /kg	Bentonite /kg	Sand /kg	Cobblestone/ kg
WB075	0.75	0.50	307.50	150	180	80	666.25	666.25
WB087	0.87	0.50	356.70	150	180	80	641.65	641.65
WB100	1.00	0.50	400	150	180	70	625	625
S04	1.00	0.40	370	120	180	70	524	786
S05	1.00	0.50	370	120	180	70	655	655
S06	1.00	0.60	370	120	180	70	786	524
CL180	0.87	0.50	322	120	180	70	655	655
CL220	0.87	0.50	357	120	220	70	641.5	641.5
CL260	0.87	0.50	391	120	260	70	604.5	604.5
B40	0.87	0.50	296	120	180	40	707	707
B70	0.87	0.50	322	120	180	70	655	655
B100	0.87	0.50	348	120	180	100	651	651

*WB: water binder ratio, S: sand ratio, CL: clay, B: Bentonite.

3 Test Results and Analysis

3.1 Triaxial compressive strength and stress-strain curve characteristics of plastic concrete

The results of the triaxial compression test of the test piece and the typical stress-strain curves under different confining pressures are shown in Table 2 and Fig. 1.

It can be seen from Table 2 that the plastic concrete triaxial compressive strengths with different mixing ratios are relatively different, and different confining pressure conditions have little effect on the concrete strength. It can be seen from Fig. 1 that the three-axis compressive stress-strain curve under the condition of constant lateral pressure can be divided into two sections, namely the curve rising section and the horizontal section. When the three-way pressure is applied, the deformation of the specimen increases rapidly. However, as the pressure continues to increase, the principal stress gradually increases, and the lateral compressive stress constrains the lateral deformation of the plastic concrete. The generation and extension of cracks are delayed by the lateral constraint, the growth of the main strain becomes relatively slow, and the slope of the stress-strain curve increases. When the principal stress gradually increases to a large stress value, the plasticity of the plastic concrete specimen at this time the deformation begins to develop gradually, the strain increases rapidly, and the stress growth is slow. The corresponding stress-strain curve rises gently and the slope gradually decreases. When the stress-strain curve reaches the peak point, the test piece reaches the triaxial compressive strength and stress. It remains basically stable, the strain continues to increase, the stress-strain curve enters the horizontal section, and the principal stress $\sigma_3$maintains the triaxial compressive strength.

Table 2 — Plastic concrete triaxial compressive strength.

Number	triaxial compressive strength / MPa		
	(0.2q,0.4q)	(0.4q,0.6q)	(0.4q,0.8q)
WB075	12.18	13.73	13.50
WB087	10.41	10.46	10.85
WB100	8.97	8.79	8.72
S04	7.38	7.49	7.54
S05	6.07	7.32	7.71
S06	7.90	8.43	8.54
CL180	8.63	10.16	10.57
CL220	9.04	9.82	10.40
CL260	6.50	7.59	6.93
B40	9.93	11.37	8.87
B70	8.63	10.16	10.57
B100	8.25	9.54	10.07

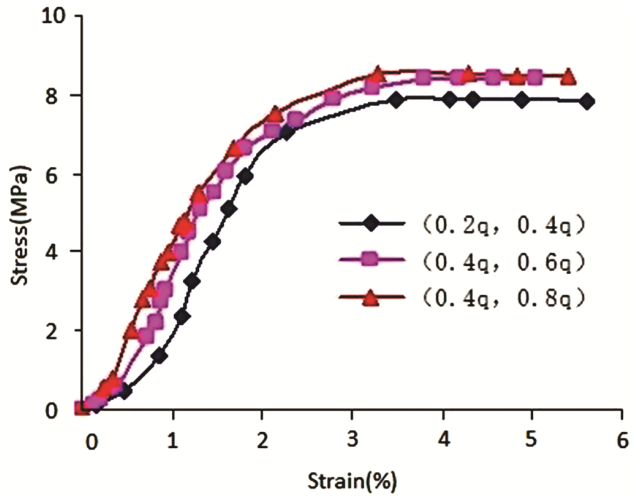

Fig. 1 — Stress-strain curves of plastic concrete under triaxial compression with constant lateral pressure.

3.2 Mathematical model of constitutive relation of plastic concrete under triaxial compression

Plastic concrete is a typical nonlinear material. The linear elastic constitutive relation cannot reflect the basic law that the strain of plastic concrete increases nonlinearly with the increase of stress. The mathematical form of the inelastic constitutive model is obscure and the derivation process is tedious. Some models require many parameters which are difficult to be calibrated accurately, so they are not easy to be accepted and applied by engineering field. In this chapter, a mathematical model of stress-strain relation of plastic concrete under triaxial compression with fixed lateral pressure is proposed by using the form of four polynomial equations.

3.2.1 The relationship between the peak secant modulus and the peak stress

It has been shown that there is a certain relationship between the elastic modulus and the strength of concrete, showing a tendency to increase with the increase of strength, but the dispersion is large. According to the statistical analysis of the test results and the influence of the minimum confining pressure and the confining pressure ratio, the relationship between the compressive peak secant modulus and the peak stress of the plastic concrete under triaxial compression can be expressed a:

$$E_f = a_1\sigma_{3f} - a_2 \quad \ldots (1)$$

Where $a_1 = 32.075\sigma_1 - 37.746\frac{\sigma_1}{\sigma_2} + 55.522$, $a_2 = -333.45\sigma_1 + 387.36\frac{\sigma_1}{\sigma_2} - 253.19$, E_f is the peak elastic modulus of plastic concrete under fixed lateral pressure, σ_{3f} is the triaxial compressive strength of plastic concrete, σ_1、σ_2 are lateral compressive stress of plastic concrete.

According to the empirical equation of uniaxial compression modulus proposed by the American Standard (ACI318-08) and the former Soviet Union specification and the Chinese standard (GB50010-2002) , the plastic concrete test data were fitted based on the stress-strain curve equation of concrete under uniaxial compression. The empirical equation for the elastic modulus of the peak secant of the plastic concrete under fixed lateral pressure is obtained as:

$$E_f = b_1\sqrt{\sigma_{3f}} + b_2 \quad \ldots (2)$$

Where $b_1 = 302.7\sigma_1 - 199.8\frac{\sigma_1}{\sigma_2} + 283.69$,

$$b_2 = -947.25\sigma_1 + 641.04\frac{\sigma_1}{\sigma_2} - 600.03.$$

$$E_f = \frac{10^5}{c_1 + \frac{c_2}{\sigma_{3f}}} \quad \ldots (3)$$

Where $c_1 = 17426.5\sigma_1 - 10747.2\frac{\sigma_1}{\sigma_2} + 4817.2$,

$$c_2 = -1913.15\sigma_1 + 910.32\frac{\sigma_1}{\sigma_2} + 40.52.$$

When the confining pressure is (0.4q, 0.6q), the average value, the mean square deviation and the coefficient of variation of the ratio between the calculated and experimental values of Eq. (1), Eq. (2) and Eq. (3) are shown in Table 3.

The average value, the mean square deviation and the coefficient of variation of the ratio between the calculated and experimental values of Eq. (1), Eq. (2) and Eq. (3) are shown in Table 4.

It can be seen from Table 3 and Table 4 that the fitting effect of Eq. (3) is better than that of Eq. (1) and (2), and the calculation of the peak secant modulus is suggested by Eq. (3).

Table 3 — The comparison between calculated values of elastic modulus and experimental values in confining pressure (0.4q, 0.6q)

Equation number	Ratio of calculated values of elastic modulus to experimental ones		
	Average value	Mean square deviation	Coefficient of variation
(1)	1.0178	0.1478	0.1452
(2)	1.0177	0.1524	0.1497
(3)	0.9993	0.1390	0.1391

3.2.2 Mathematical model of constitutive relation of plastic concrete under triaxial compression

The stress-strain curve of the plastic concrete is fitted by the theoretical mathematical model. It is found that the quartic polynomial model agrees well with the measured curve. Therefore, the quartic polynomial mathematical model of stress-strain relation of plastic concrete under triaxial compression is put forward in this paper. That is:

$$y = Ax^4 + Bx^3 + Cx^2 + Dx \ (x \le 1) \quad \ldots (4)$$

$$y = 1 (x > 1) \quad \ldots (5)$$

Where vertical and horizontal coordinates are $y = \sigma_3/\sigma_{3f}$, $x = \varepsilon_3/\varepsilon_{3f}$. ε_{3f} is the peak compressive strain corresponding to σ_{3f}.

When $\varepsilon_3 = \varepsilon_{3f}$, $\sigma_3 = \sigma_{3f}$, that is, $x = 1$, $y = 1$. Substituting $x = 1$and $y = 1$ into Eq. (4) yields:

$$A + B + C + D = 1 \quad \ldots (6)$$

Both sides of the Eq. (4) make a derivative of ε_3, then:

$$\frac{dy}{d\varepsilon_3} = (4Ax^3 + 3Bx^2 + 2Cx + D)\frac{dx}{d\varepsilon_3}$$

$$\frac{1}{\sigma_{3f}}\frac{d\sigma_3}{d\varepsilon_3} = (4Ax^3 + 3Bx^2 + 2Cx + D)\frac{1}{\varepsilon_{3f}}$$

Substituting $\varepsilon_3 = 0$, that is, x=0 into the equation:

$$\left.\frac{d\sigma_3}{d\varepsilon_3}\right|_{\varepsilon_3=0} = \frac{\sigma_{3f}}{\varepsilon_{3f}}D$$

$$D = \frac{E_0'}{E_f} \quad \ldots (7)$$

Where $E_o'$is initial tangential elastic modulus of plastic concrete under triaxial compression and $E_0' = \left.\frac{d\sigma_3}{d\varepsilon_3}\right|_{\varepsilon_3=0}$.

It can be seen from Eq. (7) that the model coefficients D are related to E_o'/E_f. Similarly, there

Table 4 — The comparison between calculated values of elastic modulus and experimental values

Equation number	Ratio of calculated values of elastic modulus to experimental ones		
	Average value	Mean square deviation	Coefficient of variation
(1)	1.0604	0.2787	0.2628
(2)	1.0624	0.2841	0.2675
(3)	0.9992	0.2437	0.2439

is a close relationship between the model coefficients A, B, C and E_o'/E_f. The initial tangential elastic modulus E_o' is difficult to measure in the statistical analysis, so the measured uniaxial elastic modulus E_0 is used instead of E_o'. E_f is calculated using Eq. (3). The curve equation of each specimen can be obtained by fitting based on the measured stress-strain curves, resulting in 33 values of A, B, C, D. And then these values are fitted to get equations of A, B, C, D as follows:

$$A = -0.1756\left(\frac{E_0}{E_f}\right)^2 + 1.6224\frac{E_0}{E_f} - 0.1773 \quad \ldots (8)$$

$$B = 0.1583\left(\frac{E_0}{E_f}\right)^2 - 1.0175\frac{E_0}{E_f} - 7.0733 \quad \ldots (9)$$

$$C = 0.1237\left(\frac{E_0}{E_f}\right)^2 - 1.8488\frac{E_0}{E_f} + 11.294 \quad \ldots (10)$$

$$D = -0.1064\left(\frac{E_0}{E_f}\right)^2 + 1.2452\frac{E_0}{E_f} - 3.0482 \quad \ldots (11)$$

E_0 is the uniaxial compressive elastic modulus of plastic concrete with 90d age.

3.3 Verify the fourth-order polynomial mathematical model

In order to verify the reliability of the mathematical model established, the experimental measured curves of the test pieces of each group are compared with the theoretical model curves obtained by using Eqs (4) and (5), as shown in Figs 2 – 12. From the comparison of the theoretical model curve and the experimental measured curve in Figs (2 – 12), it can be seen that the theoretical model curve under the lateral confining pressure of (0.4q, 0.6q) almost coincides with the measured curve, (0.2q, 0.4q), (0.4q, 0.8q) There is a slight deviation between the theoretical curve and the measured curve under the lateral confining pressure, but the overall consistency is consistent, which fully proves that the established polynomial mathematical model has good reliability.

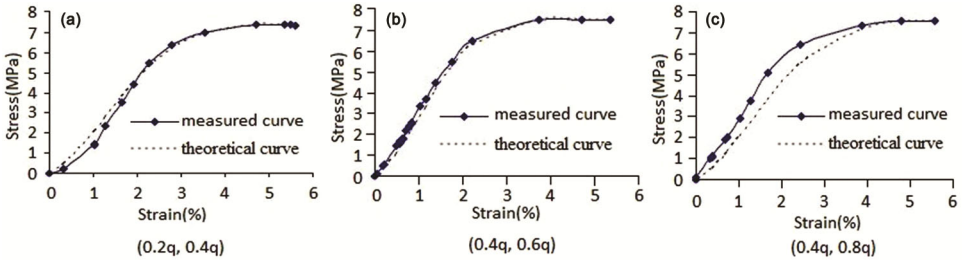

Fig. 2 — The Comparison between theoretical curves and measured curves of S04 models.

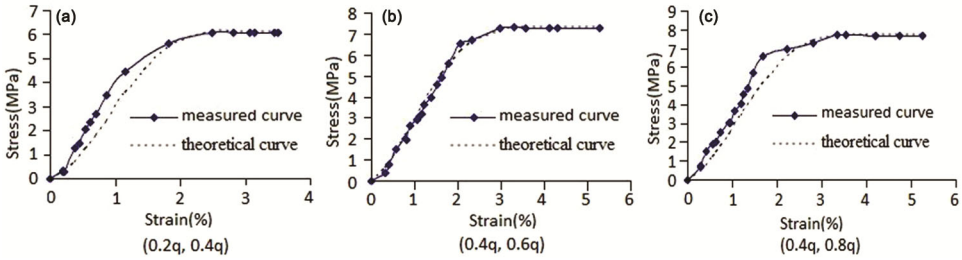

Fig. 3 — The Comparison between theoretical curves and measured curves of S05 models.

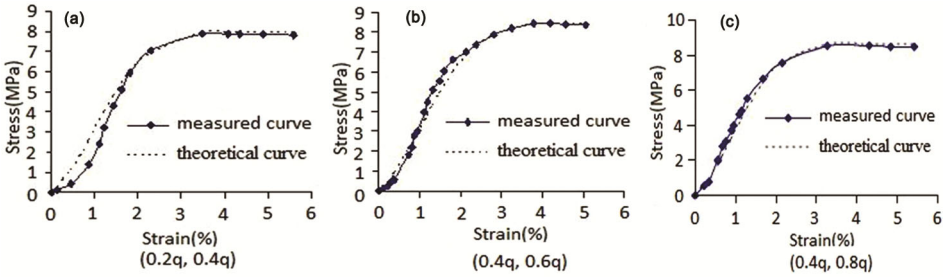

Fig. 4 — The Comparison between theoretical curves and measured curves of S06 models.

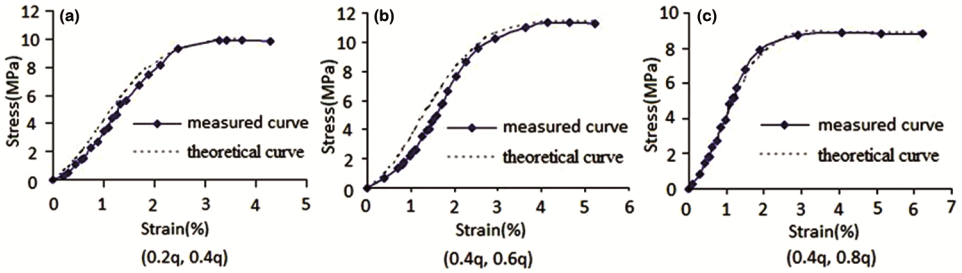

Fig. 5 — The Comparison between theoretical curves and measured curves of B40 models.

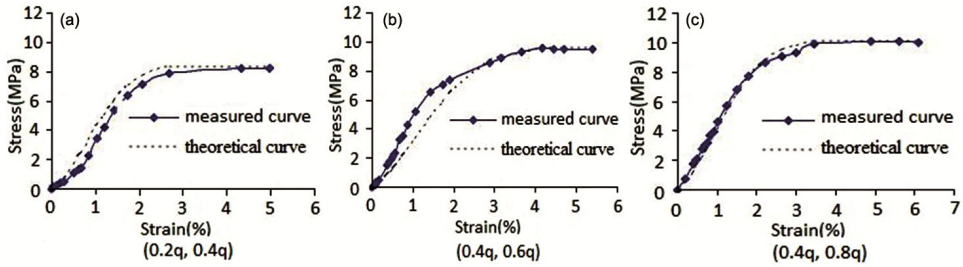

Fig. 6 — The Comparison between theoretical curves and measured curves of B100 models.

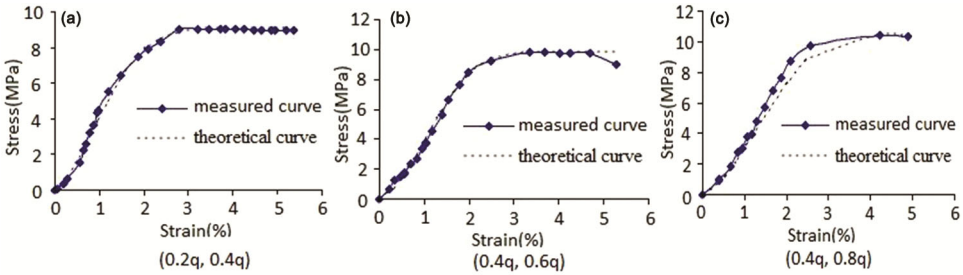

Fig. 7 — The Comparison between theoretical curves and measured curves of CL220 models.

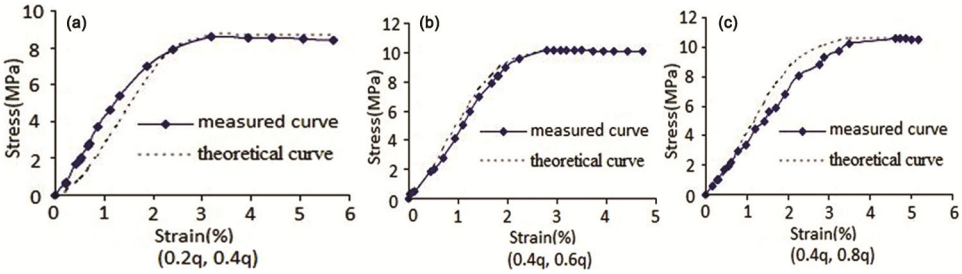

Fig. 8 — The Comparison between theoretical curves and measured curves of CL180、B70

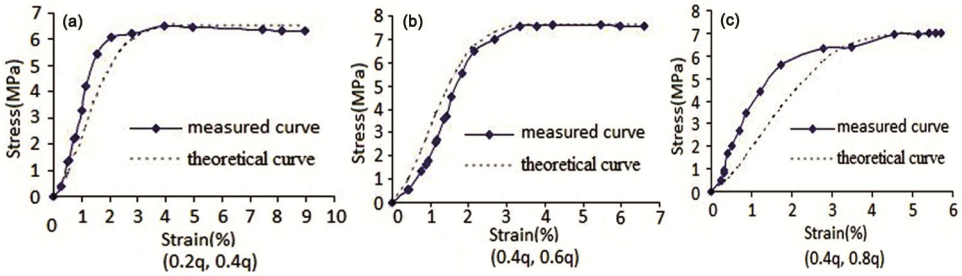

Fig. 9 — The Comparison between theoretical curves and measured curves of CL260 models.

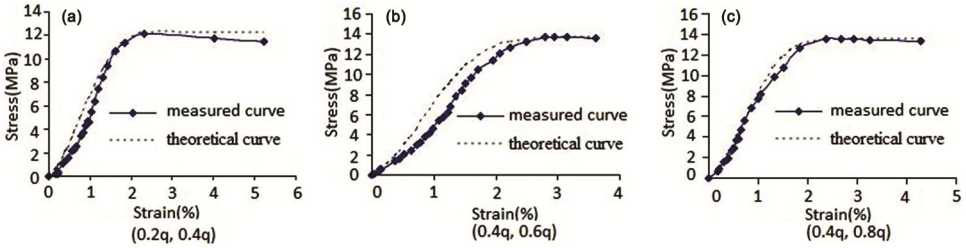

Fig . 10 — The Comparison between theoretical curves and measured curves of WB075 models.

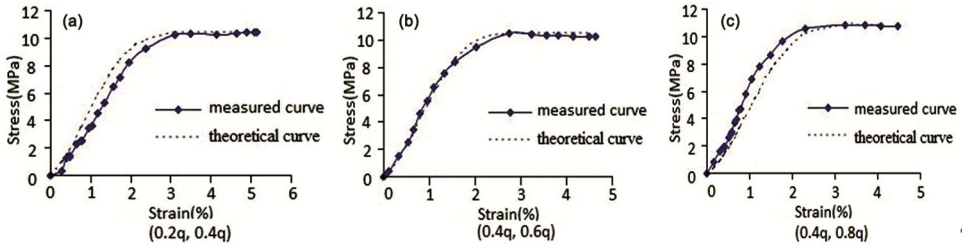

Fig. 11 — The Comparison between theoretical curves and measured curves of WB087 models.

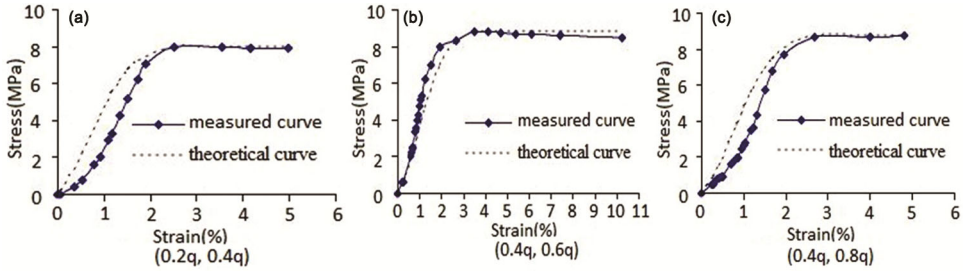

Fig. 12 — The Comparison between theoretical curves and measured curves of WB100 models.

4 Conclusions

(i) The slope of the 540 d plastic concrete in the rising section of the stress-strain curve under the medium-high lateral confining pressure is larger than the low confining pressure, but the compressive strength is not much different.

(ii) Refer to different specifications to obtain the calculation formula of the compressive peak secant modulus of plastic concrete. After comparison, it is recommended that the triaxial compression peak secant modulus be calculated by formula (3).

(iii) A quadratic polynomial mathematical model conforming to the triaxial compression constitutive relation of plastic concrete is fitted, and the model has good reliability.

Acknowledgment

This work was supported by National Natural Science Foundation of China (Project No. 50979100). The study received helpful assistance from College of water resources and environment, Zhengzhou University, and North China University of Water Resources and Electric Power. Thanks to anonymous commentators for providing valuable advice to this manuscript.

References

1 Hu L M, *Stress-strain relation model and failure criterion of plastic concrete under compression*, Doc Diss of Zhengzhou Univ, (2012).
2 Gao D Y & Song S Q, *J Hydraul Eng*, 47 (2016) 10.
3 Gao D Y, Song S Q & Yang L, J Hydraul Eng, 45 (2014) 360.
4 Yao J W, *Build Sci*, 27 (2011) 28.
5 Launay P & Gachon H, *J Am Concr Inst*, 1 (1970) 269.
6 Song Y P, *Constitutive relation and failure criterion of various concrete materials*, 1st Edn, China Water Conserv and Hydropower Press, Beijing, 2002.
7 Mahboubi A & Ajorloo A, *Cem Concr Res*, 35 (2005) 412.
8 Nicholas T & Chen S E, *Mode I Fatigue of the Carbon fiber-Reinforced Plastic-Concrete Interface Bond*, Experimental Techniques. (2011).
9 Hinchberger S, Weck J & Newson T, *J Can Geotech*, 47 (2010) 461.
10 Mahboubi A & Ajorloo A, *Cem Concr Res*, 35 (2005) 412.

11 Detwiler R, Folliard K & Olek J, Causes and Prevention of Crack evelopment in Plastic Concrete, *Portland Cement Association Annual Meeting*, (2008) 130.
12 Morris P H & Dux P F, *ACI Mater J*, 103 (2006) 90.
13 Sadrekarimi J, *J Inst Eng*, 82 (2002) 201.
14 ICOLD, *Filling materials for watertight cutoff walls. International Committee of Large Dams*: Paris, Bulletin, 51 (1985).
15 Deng M J, *Study on the performance of plastic concrete cutoff wall for enclosing dam* in East Pinghu. Doc Diss Of Tsinghua Univ, (2005).
16 Wang X Z, Experimental study on plastic concrete cutoff wall Doc Diss Of Nanchang Univ, (2005).
17 Shi Y, Chen X & Li J Z, *J Yangtze River Sci Res Inst*, 1 (2019) 3.
18 Song S Q, Chen Y J & Han Y, *J Hydroelectric Eng*, 37 (2018) 58.
19 Liu L L, Chang F F & Xie W, *J Yangtze River Sci Res Inst*, 32 (2015) 116.
20 China Build Mater Sci Res Inst, Ordinary Portland cement, (GB175-2007). China Stan, Press, Beijing, 2007.
21 China Assoc of Sand and Gravel, Sand for construction, (GB/T14684—2011) China Stan, Press, Beijing, 2011.
22 China Three Gorges Corp ,Specifications for hydraulic concrete construction, (DL/T5144—2001), China Power Press, Beijing, 2002.